Available online at www.sciencedirect.com

ScienceDirect

IFAC Papers Online CONFERENCE PAPER ARCHIVE

IFAC PapersOnLine 56-2 (2023) 7710–7715

Population-Dynamics-Assisted Coalitional Model Predictive Control for Parabolic-Trough Solar Plants ⋆

Ana Sánchez-Amores *, **Juan Martinez-Piazuelo** **, **José M. Maestre** *, **Carlos Ocampo-Martinez** **, **Eduardo F. Camacho** *, **Nicanor Quijano** ***

* *Systems and Automation Engineering Department, University of Seville, Spain (e-mail: {asamores, pepemaestre, efcamacho}@us.es).*
** *Automatic Control Department, Universitat Politècnica de Catalunya, Spain (e-mail: {juan.pablo.martinez.piazuelo, carlos.ocampo}@upc.edu).*
*** *Departamento de Ingeniería Eléctrica y Electrónica, Universidad de los Andes, Colombia (e-mail: nquijano@uniandes.edu.co).*

Abstract: This paper proposes a coalitional model predictive control method for temperature regulation in parabolic-trough solar fields. The global optimization problem is divided into a set of local subproblems that will be solved in parallel by a set of coalitions. However, these local (smaller) problems remain coupled by a common global resource constraint. In this regard, we present a population-dynamics-assisted resource allocation approach to fully decouple the local optimization problems. By doing this, each coalition can address its corresponding optimization problem without relying on the solutions of the other coalitions. To illustrate the proposed methodology, we provide simulation results for a 100-loop parabolic-trough solar collector field.

Keywords: Model predictive control, coalitional control, population dynamics, distributed solar collector field

1. INTRODUCTION

The increasing levels of carbon dioxide and other greenhouse gases in the atmosphere have generated a great interest in the use of renewable energy to mitigate the severe environmental impact of fossil fuel systems. Solar, wind, geothermal, and biomass comprise different renewable energy sources. Among them, solar energy is the most abundant and has drawn the attention of the research community (Şen, 2004). Solar radiation can be used to produce electricity directly, using photovoltaic panels, or indirectly, through concentrated solar power systems. The latter concentrates sunlight to heat a fluid that will produce steam to drive turbine generators (Peinado Gonzalo et al., 2019). Within this technology, we will focus on the control for parabolic-trough collector (PTC) solar plants (Gálvez-Carrillo et al., 2009).

Unlike other power generation processes where we can manipulate the main energy source, solar energy acts as a disturbance from a control view point. In this framework, model predictive control (MPC) deals with system disturbances and constraints in a receding-horizon fashion, which makes it a suitable control strategy for parabolic trough plants. However, one of the main limitations of this approach is that it solves an optimization problem in real-time at each time step, requiring a great computational effort when solving large-scale optimization problems. Nowadays, there is a growing interest in developing alternative MPC strategies that reduce the computational burden regarding the implementation of a centralized approach in parabolic-trough plants. For example, Escaño et al. (2021) formulate a fuzzy MPC to forecast the evolution of the outlet temperature of the solar plant, reducing processing times compared to the non-linear model of the field. Also, Ruiz-Moreno et al. (2021) present an approach in which artificial neural networks are trained to approximate the optimal flow value given by an MPC.

As an alternative, coalitional MPC (Maxim and Caruntu, 2022) splits the large-scale system into smaller subsystems governed by local controllers or agents. This type of distributed control dynamically groups cooperative controllers only when overall performance improves (Barreiro-Gomez and Zhu, 2022). In particular, the local subproblems in the parabolic-trough fields are coupled by a shared resource constraint related to the total amount of heat transfer fluid that circulates through the field; see Masero et al. (2020). In this regard, a key problem is how to decouple the shared constraint so that the local problem of each coalition can be solved independently of the rest of

⋆ The authors gratefully acknowledge the financial support by the European Research Council (ERC) under the European Union's Horizon 2020 research and innovation program (OCONTSOLAR, grant agreement No 789051). In addition, the authors would like to thank the projects PID2020-119476RB-I00 (C3PO-R2D2) and TED2021-129927B-I00 (MASHED) funded by MCIN/ AEI /10.13039/501100011033 and by the "European Union NextGenerationEU/PRTR" for supporting this research. Finally, Juan Martinez-Piazuelo gratefully acknowledges the Universitat Politècnica de Catalunya and Banco Santander for the financial support of his predoctoral grant FPI-UPC.

10.1016/j.ifacol.2023.10.1174

the system. To this end, this paper proposes a coalitional MPC approach where the population dynamics framework (Sandholm, 2010) is used to allocate the available resource among multiple coalitions, guaranteeing the satisfaction of the coupled constraint so that local optimization problems can be solved in a decentralized (parallel) fashion. The motivation behind such an approach is that population dynamics have some invariance and asymptotic stability features that render them suitable for dynamic resource allocation problems (Quijano et al., 2017). In particular, the invariance property can be exploited to guarantee the feasibility of the resource distribution at any point in time, while the asymptotic stability feature allows us to achieve an optimal resource distribution over time. Consequently, based on the above, the main contribution of this paper is the formulation of a novel coalitional MPC approach incorporating population-dynamics-assistance for the regulation of temperature in parabolic-through solar collector fields. The proposed method ensures the satisfaction of the shared resource constraint and provides better scalability to large-scale systems, as it reduces the overall computational burden. In addition, we evaluate the performance of the proposed approach through a numerical simulation of a 100-loop version of the ACUREX solar field of the *Plataforma Solar de Almería*, Spain. This numerical simulation shows that our proposed method requires significantly less computation time and imposes negligible losses in performance compared to the centralized solution.

The remainder of this paper is structured as follows. Section 2 provides the model of the parabolic-trough solar collector field and the operational constraints of the system. Section 3 presents the underlying control goal and describes the proposed coalitional MPC setting. In addition, we motivate the use of population dynamics to allocate the common resource constraint. Finally, results on 100-loop solar collector fields are presented in Section 4, and Section 5 concludes the paper.

2. DESCRIPTION OF THE SOLAR FIELD

A parabolic-trough collector field consists of a set of mirrors curved in a parabolic shape that concentrate solar irradiance in a receiver tube located in its focal line. A heat transfer fluid (HTF) heats up as it flows through the pipe, and therefore carries the thermal energy to produce steam. Finally, a steam turbine generates electrical energy. The field can be modeled as a set $\mathcal{L} = \{1, \dots, N\}$ of N parallel loops, where each loop consists of different collectors connected in series. In particular, we assume that we can control the HTF flow of each loop $j \in \mathcal{L}$.

2.1 Dynamical Model of the PTC field

In what follows, we consider the concentrated parameter model of a PTC field (Camacho and Gallego, 2015), which provides a lumped description of each loop. More precisely, the dynamics of the outlet temperature of a loop are given by the variation of the internal energy of the HTF. We can describe the continuous-time model for each loop $j \in \mathcal{L}$ as

$$\begin{aligned} C_j(t)\frac{dT_j(t)}{dt} =& \alpha_j \eta S I(t) - \beta_j S H_j(t)\left(\bar{T}_j(t) - T^a(t)\right) \\ & - P_j(t) q_j(t)\left(T_j(t) - T_j^{in}(t)\right), \end{aligned} \tag{1}$$

Table 1. Model's variables and parameters

Symbol	Description	Units
t	Continuous-time variable	s
k	Discrete-time index	-
T_j, T_j^{in}	Outlet and inlet temp. of loop j	ºC
T, T^{in}	Outlet and inlet temp. of the field	ºC
T^a	Ambient temperature	ºC
$\bar{T}$	Mean inlet-outlet temperature	ºC
q_j	HTF flow in loop j	l/s
q^T	Total HTF flow	l/s
I	Direct solar irradiance	W/m^2
H_j	Coef. of thermal losses of loop j	W/(m^2 ºC)
N	Number of loops	-
L	Length of each loop	m
S	Reflective surface of each loop	m^2
a_f	Cross-sectional area of the fluid	m^2
ρ	Density of the HTF	kg/m^3
c	Specific heat capacity of the HTF	J/(kg ºC)
α_j, β_j	Cleanliness and loss scale factor of j	-

with $C_j(t) = \rho_j\left(T(t)\right) c_j\left(T(t)\right) a_f L$, $\bar{T}_j(t) = 0.5\big(T_j(t) + T_j^{in}\big)$, and $P_j(t) = \rho_j\left(T(t)\right) c_j\left(T(t)\right)$.

For clarity, Table 1 summarizes the model variables and parameters. Here, the density and specific heat capacity of the HTF are temperature-dependent. Also, the global coefficient of thermal losses $H_j(t)$ depends on the outlet, inlet, and ambient temperatures. Mirrors of different collectors might have different cleanliness levels and thermal losses, consequently, loops may have different dynamics. In this regard, we consider α_j and β_j as the scale factors that characterize the cleanliness of the mirrors and the thermal losses of each loop, respectively.

2.2 System's Constraints

The direct normal irradiance (DNI), ambient temperature, and inlet temperature are considered disturbances that can be estimated or measured. Moreover, it is assumed that the inlet temperature of each loop is equal to the inlet temperature of the HTF to the field, i.e., $T_j^{in} = T^{in}$, for all $j \in \mathcal{L}$. Also, we can describe the outlet temperature of the whole field as

$$T(t) = \frac{\sum_{j=1}^{N} T_j(t) q_j(t)}{q^T(t)}, \tag{2}$$

where $q^T(t) = \sum_{j=1}^{N} q_j(t)$ is the total HTF flow.

In addition, we must restrict the operation region of the outlet temperature of each loop, as well as the values of the HTF flow of each loop $j \in \mathcal{L}$ and the entire field. Namely,

$$T^{\min} \leq T_j(t) \leq T^{\max}, \ \ \forall j \in \mathcal{L} \tag{3a}$$
$$q^{\min} \leq q_j(t) \leq q^{\max}, \ \ \forall j \in \mathcal{L} \tag{3b}$$
$$q^T(t) \leq q^{T,\max}. \tag{3c}$$

2.3 Linear Discrete-Time Model

For the control strategy described in this work, we propose a linearization of the concentrated parameter model in (1), with the goal to operate each loop $j \in \mathcal{L}$ close to its desired

operating point $\left(T_j^\circ, q_j^\circ\right)$. To this end, we can define the temperature and flow of each loop j as the sum of its value at the operating point plus a small increment represented by the deviation variables (x_j, u_j). That is,

$$T_j(t) = T_j^\circ + x_j(t), \;\; q_j(t) = q_j^\circ + u_j(t). \tag{4}$$

Based on (1) and (4), and approximating the time derivatives using the forward Euler method, we can express the discrete-time lumped model for each loop $j \in \mathcal{L}$ as

$$x_j[k+1] = A_j x_j[k] + B_j u_j[k] + w_j[k]. \tag{5}$$

Consequently, we can express the model of the field as

$$x[k+1] = Ax[k] + Bu[k] + w[k], \tag{6}$$

with

$$\begin{aligned} x[k] &= \mathrm{col}\left(x_1[k], x_2[k], \ldots, x_N[k]\right) \in \mathbb{R}^N, \\ u[k] &= \mathrm{col}\left(u_1[k], u_2[k], \ldots, u_N[k]\right) \in \mathbb{R}^N, \\ w[k] &= \mathrm{col}\left(w_1[k], w_2[k], \ldots, w_N[k]\right) \in \mathbb{R}^N, \\ A &= \mathrm{diag}\left(A_1, A_2, \ldots, A_N\right) \in \mathbb{R}^{N\times N}, \\ B &= \mathrm{diag}\left(B_1, B_2, \ldots, B_N\right) \in \mathbb{R}^{N\times N}. \end{aligned}$$

Here, col$(\cdot)$ and diag$(\cdot)$ denote the construction of a column vector and a block diagonal matrix, respectively. Besides, the constraints in (3) can be written in terms of deviation variables (4) as

$$T^{\min} - T_j^\circ \le x_j[k] \le T^{\max} - T_j^\circ, \;\; \forall j \in \mathcal{L} \tag{7a}$$

$$q^{\min} - q_j^\circ \le u_j[k] \le q^{\max} - q_j^\circ, \;\; \forall j \in \mathcal{L} \tag{7b}$$

$$\sum_{j\in\mathcal{L}} u_j[k] \le q^{T,\max} - \sum_{j\in\mathcal{L}} q_j^\circ. \tag{7c}$$

3. CONTROL PROBLEM AND PROPOSED METHOD

As mentioned above, the overall control objective is to regulate the deviation variables (4) so that the global system (6) remains close to the desired operating point (T_j°, q_j°), for all $j \in \mathcal{L}$, while satisfying the constraints given in (7). This overall objective is formalized as follows.

Definition 1. (Control Objective) The model predictive control problem to be solved at time k is given by

$$\min_{\mathbf{u}[k]} \sum_{n=1}^{N_\mathrm{p}} x[k+n]^\top Q x[k+n] + \sum_{n=0}^{N_\mathrm{p}-1} u[k+n]^\top R u[k+n], \tag{8}$$

subject to the constraints (6) and (7), where the prediction horizon is denoted as $N_\mathrm{p} \in \mathbb{Z}_{\ge 1}$. Here, the weighting matrices $Q, R \in \mathbb{R}^{N\times N}$ are symmetric positive definite, and the vector $\mathbf{u}[k]$ provides the sequence of inputs $u[\cdot]$ from the time instants $n = k$ to $k + N_\mathrm{p} - 1$, that is, $\mathbf{u}[k] = \mathrm{col}\left(u[k], u[k+1], \ldots, u[k+N_\mathrm{p}-1]\right)$.

Assumption 1. The set of solutions to the problem in Definition 1 is not empty. Also, $Nq^{\min} \le q^{T,\max} \le Nq^{\max}$.

If the solar field is sufficiently large, then the application of centralized methods to solve the problem in Definition 1 may be unfeasible for real-time control. To overcome this issue, we propose a coalitional control approach in which the centralized controller is replaced by a set of local controllers that will solve their optimization problems independently, leading to a lower computational cost.

3.1 Coalitional Control Approach

We consider the graph $\mathcal{G} = (\mathcal{L}, \mathcal{E})$, where $\mathcal{L}$ is the set of loops and $\mathcal{E} \subseteq \mathcal{L} \times \mathcal{L}$ is the set of bidirectional communication links that allow the controllers of the different loops to exchange data.

Assumption 2. At any time, the graph $\mathcal{G}$ is partitioned into a set of M disjoint complete subgraphs $\mathcal{G}_1, \mathcal{G}_2, \ldots, \mathcal{G}_M$. For every $i \in \{1, 2, \ldots, M\}$ we have $\mathcal{G}_i = (\mathcal{L}_i, \mathcal{E}_i)$, with $\mathcal{L}_i \subseteq \mathcal{L}$ and $\mathcal{E}_i = \mathcal{L}_i \times \mathcal{L}_i$. Also, $\mathcal{L}_i \cap \mathcal{L}_\ell = \emptyset$ holds for all $i \neq \ell$, and $\mathcal{L}_1 \cup \mathcal{L}_2 \cup \cdots \cup \mathcal{L}_M = \mathcal{L}$.

Definition 2. (Coalition) Under the partition provided by Assumption 2, a coalition $\mathcal{C}_i = \mathcal{L}_i$ is a subset of loops whose controllers are connected through a set of links $\mathcal{E}_i$ according to the (complete) subgraph $\mathcal{G}_i$. Thus, agents within the same coalition operate as a single entity, and the size of a coalition can range from a singleton $\mathcal{C}_i = j$, i.e., $|\mathcal{C}_i| = 1$, to the grand coalition $\mathcal{C}_i = \mathcal{L}$, i.e., $|\mathcal{C}_i| = N$, where $|\mathcal{C}_i|$ denotes the cardinality of $\mathcal{C}_i$. Throughout, we let $\mathcal{P} = \{\mathcal{C}_1, \mathcal{C}_2, \ldots, \mathcal{C}_M\}$ be the set of coalitions, so that $\mathcal{P}$ characterizes the partition of the system.

Remark 1. Loops can be grouped using different criteria such as geographical proximity, solar irradiance, or HTF flow requirements (Masero et al., 2020). In this paper, we do not focus on a specific partitioning method, instead, we assume that the partition is given by an arbitrary criterion.

Based on the partition $\mathcal{P}$, we let $q_{\mathcal{C}_i}^{\max}$ be the maximum HTF flow allowed for coalition $\mathcal{C}_i \in \mathcal{P}$, and these maximum coalition-level flows are set to guarantee $\sum_{i=1}^{M} q_{\mathcal{C}_i}^{\max} = q^{T,\max} - \sum_{j\in\mathcal{L}} q_j^\circ$ (the details on how to compute $q_{\mathcal{C}_i}^{\max}$ for each coalition are given in Section 3.2). Expressed in the deviation variables, it is then required that

$$\sum_{j\in\mathcal{C}_i} u_j[k] \le q_{\mathcal{C}_i}^{\max}, \quad \forall \mathcal{C}_i \in \mathcal{P}. \tag{9}$$

Clearly, if the constraint in (9) holds for all coalitions, then the overall field-level constraint in (7c) holds as well.

Definition 3. (Local Control Objective) The model predictive control problem to be solved at time k by coalition $\mathcal{C}_i \in \mathcal{P}$ is given by

$$\min_{\mathbf{u}_{\mathcal{C}_i}[k]} \sum_{n=1}^{N_\mathrm{p}} \sum_{j\in\mathcal{C}_i} x_j^2[k+n] Q_j + \sum_{n=0}^{N_\mathrm{p}-1} \sum_{j\in\mathcal{C}_i} u_j^2[k+n] R_j, \tag{10}$$

subject to (5), (7a), and (7b), for all $j \in \mathcal{C}_i$, and (9). Here, the (local) weighting scalars $Q_j, R_j \in \mathbb{R}_{\ge 0}$ are set according to the global weighting matrices in (8), for all $j \in \mathcal{C}_i$; the vector $\mathbf{u}_{\mathcal{C}_i}[k]$ describes the sequence of inputs within a coalition $\mathcal{C}_i$ from instants $n = k$ to $k + N_\mathrm{p} - 1$; and the vector $u_{\mathcal{C}_i}[\cdot] = \mathrm{col}\left(\{u_j[\cdot]\}_{j\in\mathcal{C}_i}\right)$ is comprised of the inputs of the loops belonging to coalition $\mathcal{C}_i$.

We highlight that once the $q_{\mathcal{C}_i}^{\max}$ term is computed for each coalition, the local control problems in Definition 3 are decoupled over the multiple coalitions. In this way, each coalition's local controller can solve the problem in (10) in a decentralized manner.

3.2 Resource Allocation via Population Dynamics

In this section, we formulate the proposed population dynamics-assisted resource allocation method that is used

to determine $q_{\mathcal{C}_i}^{\max}$ for each coalition $\mathcal{C}_i \in \mathcal{P}$. To this end, we consider a model predictive control problem with unitary control horizon as defined next.

Definition 4. (Control Objective under Unitary Control Horizon) The unitary control horizon model predictive control problem to be solved at time k is given by

$$v[k] = \arg\min_{u[k]} \sum_{n=1}^{N_\mathrm{p}} x[k+n]^\top Q x[k+n] + \sum_{n=0}^{N_\mathrm{p}-1} u[k]^\top R u[k], \tag{11}$$

subject to the constraints in (6), (7b), and the coupled constraint $\sum_{j\in\mathcal{L}} u_j[k] = q^{T,\max} - \sum_{j\in\mathcal{L}} q_j^\circ$. Here, the weighting matrices for state and input, namely Q and R, are the same ones considered in Definition 1.

The solution of the problem in Definition 4 gives an estimate of the average flow of HTF required by each loop over N_p, and thus provides information to determine $q_{\mathcal{C}_i}^{\max}$ for each coalition $\mathcal{C}_i \in \mathcal{P}$. Compared to the problem in Definition 1, the one in Definition 4 regards the constraint in (7c) with strict equality, and disregards the constraints in (7a) (nevertheless, recall that the constraints in (7a) are still considered at each coalition's local controller). We enforce (7c) with strict equality to allocate the totality of the available resource over the multiple coalitions, so that $\sum_{i=1}^{M} q_{\mathcal{C}_i}^{\max} = q^{T,\max} - \sum_{j\in\mathcal{L}} q_j^\circ$. On the other hand, we remove the constraints in (7a) to guarantee the non-emptiness of the set of solutions under the unitary control horizon constraint.

Now, according to the dynamics in (6), the state $x[k+n]$ under a constant $u[k]$ applied during times $k, k+1, \ldots, k+n-1$ is given by $x[k+n] = A^n x[k] + G_n u[k] + d[k+n-1]$, where $G_n = \sum_{\ell=0}^{n-1} A^\ell B$ and $d[k+n-1] = \sum_{\ell=0}^{n-1} A^\ell w[k+n-1-\ell]$. Consequently, the cost function in (11) can be equivalently written as

$$\begin{aligned} J(u[k]) = \sum_{n=1}^{N_\mathrm{p}} \Big(& x[k]^\top A^{n\top} Q A^n x[k] + 2x[k]^\top A^{n\top} Q G_n u[k] \\ & + 2x[k]^\top A^{n\top} Q d[k+n-1] + u[k]^\top G_n^\top Q G_n u[k] \\ & + 2u[k]^\top G_n^\top Q d[k+n-1] \\ & + d[k+n-1]^\top Q d[k+n-1] \Big) + N_\mathrm{p} u[k]^\top R u[k]. \end{aligned}$$

Besides, the gradient of $J(\cdot)$ with respect to $u[k]$ is given by $g(u[k]) = \sum_{n=1}^{N_\mathrm{p}} \Big(2G_n^\top Q A^n x[k] + 2G_n^\top Q G_n u[k] + 2G_n^\top Q d[k+n-1] \Big) + 2N_\mathrm{p} R u[k]$. Based on these formulations, to solve the problem in Definition 4 we consider the iterative dynamics given by

$$\vartheta_j[\kappa] = \max\left(q^{\max} - q^{\min} - \bar{v}_j[\kappa], 0\right) \tag{12a}$$

$$\varrho_{ij}[\kappa] = \min\left(\max\left(g_i\left(\bar{v}[\kappa]\right) - g_j\left(\bar{v}[\kappa]\right), 0\right), \gamma\right) \tag{12b}$$

$$\mu_j[\kappa] = \sum_{i\in\mathcal{L}} \left(\bar{v}_i[\kappa]\vartheta_j[\kappa]\varrho_{ij}[\kappa] - \bar{v}_j[\kappa]\vartheta_i[\kappa]\varrho_{ji}[\kappa]\right) \tag{12c}$$

$$\bar{v}_j[\kappa+1] = \bar{v}_j[\kappa] + \epsilon\mu_j[\kappa] \tag{12d}$$

$$v_j[\kappa] = \bar{v}_j[\kappa] + q^{\min} - q_j^\circ, \tag{12e}$$

for all $i, j \in \mathcal{L}$, where $\gamma, \epsilon \in \mathbb{R}_{>0}$ are strictly positive constants whose values are defined in Theorem 1, and the initial condition $\bar{v}[0] = \mathrm{col}\left(\bar{v}_1[0], \bar{v}_2[0], \ldots, \bar{v}_N[0]\right)$ satisfies

$$\bar{v}[0] \in \left\{ \bar{v} \in \mathbb{R}^N_{\geq 0} : \begin{array}{l} \sum_{j\in\mathcal{L}} \bar{v}_j = q^{T,\max} - Nq^{\min} \\ \bar{v}_j \leq q^{\max} - q^{\min}, \quad \forall j \in \mathcal{L} \end{array} \right\}. \tag{13}$$

Note that the updates in (12) occur at discrete-time instants κ, which are not necessarily equal to the time instants k of the discrete-time model in (6). Based on the dynamics in (12) and the partition $\mathcal{P}$, the resource allocation at time κ is computed as

$$q_{\mathcal{C}_i}^{\max}[\kappa] = \sum_{j\in\mathcal{C}_i} v_j[\kappa], \quad \forall \mathcal{C}_i \in \mathcal{P}. \tag{14}$$

The iterative dynamics in (12) correspond to a discretization of the so-called Smith population dynamics with carrying capacities (Barreiro-Gomez and Tembine, 2018). As mentioned above, our interest on the dynamics in (12) is due to their invariance and asymptotic stability properties, which are formalized in Theorem 1.

Theorem 1. Consider the iterative dynamics in (12) with $\gamma = 2\left(q^{T,\max} - Nq^{\min}\right)\lambda_{\max}\left(\sum_{n=1}^{N_\mathrm{p}} G_n^\top Q G_n + N_\mathrm{p} R\right)$ and $0 < \epsilon < \left(\gamma\left(q^{\max} - q^{\min}\right)(N-1)\right)^{-1}$ (here, $\lambda_{\max}(\cdot)$ denotes the maximum eigenvalue of the corresponding matrix). Moreover, let $\bar{v}[0]$ satisfy the condition in (13). Then, the following facts hold.

(1) For all $\kappa \geq 0$, the vector $v[\kappa]$ satisfies the constraints of the problem in Definition 4.
(2) The set of solutions of the problem in Definition 4 is asymptotically stable under the considered dynamics.
(3) For all $\kappa \geq 0$, if $v[\kappa]$ is not a solution of the problem in Definition 4, then $J(v[\kappa+1]) < J(v[\kappa])$.

Proof 1. See Martinez-Piazuelo et al. (2022).

According to Theorem 1, if the constraint in (13) is satisfied, then the feasible set of the problem in Definition 4 is forward-time invariant under the dynamics in (12), implying that the resource allocation in (14) always satisfies $\sum_{i=1}^{M} q_{\mathcal{C}_i}^{\max} = q^{T,\max} - \sum_{j\in\mathcal{L}} q_j^\circ$, as desired. Furthermore, the cost function in (11) strictly decreases under the trajectories of the dynamics in (12), and its minimizer is achieved asymptotically. These facts show that, regardless of the number of update iterations applied to the dynamics in (12), the corresponding resource allocation is always better than the initial one (in the sense of the problem in Definition 4). Clearly, such a property is attractive when the updates in (12) can only be executed a limited amount of times due to real-time constraints, as is our case.

In summary, the overall proposed coalitional approach is composed of two layers. At the top layer, the field partition $\mathcal{P}$ is computed, and the population-dynamics-assisted resource allocation method is employed to allocate the resource $q_{\mathcal{C}_i}^{\max}$ to each coalition $\mathcal{C}_i \in \mathcal{P}$. At the bottom layer, on the other hand, the controller of each coalition $\mathcal{C}_i \in \mathcal{P}$ solves the local model predictive control problem of Definition 3 subject to the resource allocation provided by the top layer.

4. NUMERICAL SIMULATIONS

Here, we provide simulation results on a 100-loop parabolic-trough solar plant. The control objective is to operate the plant around a desired temperature of 250°C, while satisfying the operational constraints. In this regard, the

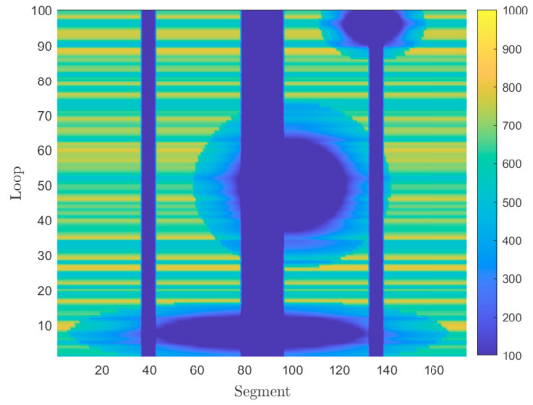

Fig. 1. Representation of the effective DNI profile of the 100-loop collector field at $t = 45$min.

values of the parameters in (3) are set as $T^{\min} = 220°$C, $T^{\max} = 300°$C, $q^{\min} = 0.2$ l/s, $q^{\max} = 1.5$ l/s, and $q^{T,\max} = 53.88$ l/s. We highlight that the maximum flow value corresponds to the total HTF flow at the desired operating point of the system.

The results obtained with the proposed coalitional approach are compared with those obtained with the centralized MPC that solves the optimization problem in Definition 1, and we also compare the proposed approach with an alternative coalitional scheme in which the maximum flow of a coalition is calculated as the sum of the flow values at the operating point of the different loops within the coalition, that is,

$$q^{\max}_{\mathcal{C}_i} = \sum_{j \in \mathcal{C}_i} q^{\circ}_j, \ \forall \mathcal{C}_i \in \mathcal{P}, \tag{15}$$

Let us define $\mathbf{P} = \sum_{k=1}^{T_{\text{sim}}} \|T[k] - T^{\circ}\|_{\hat{Q}} + \|q^T[k] - q^{T,\circ}\|_{\hat{R}}$ as the index that measures the performance of a given control algorithm throughout the simulation, where the simulation length is set to $T_{\text{sim}} = 90$min, and $\hat{Q}$ and $\hat{R}$ are positive weighting scalars. Moreover, to compare the required computational load of different control strategies, we measure the average computation time in the simulation, as well as the standard deviation of the sample.

Case of study: ACUREX Solar Plant

Here, we study the ACUREX parabolic-trough solar collector field located in *Plataforma Solar de Almería* (PSA), Spain. For this plant, Therminol 55 is used as the HTF, whose density (ρ) and specific heat capacity (c) are given by (Camacho et al., 1997): $\rho\,(T_f(t)) = 903 - 0.672 T_f(t)$ and $c\,(T_f(t)) = 1820 + 3.478 T_f(t)$, where $T_f(t)$ is the temperature of the HTF at time instant t. While the original field is modeled as a set of $N = 10$ parallel loops of 174m length, in what follows we consider a 100-loop extension of this plant, and we distinguish the active part that receives solar irradiance (142m length) from the passive one where solar radiation does not reach (30m length). For our simulations, the values of the parameters of the system (1) are defined as $L = 174$ m, $S = 267.4$ m^2, $a_f = 7.55 \cdot 10^{-4}$ m^2, $\eta = 0.64$, $\alpha_j \in [0.6,\ 1]$ and $\beta_j \in [1,\ 1.25]$.

We provide two results of our proposed approach using different criteria to calculate the partition of the field. In this regard, we will calculate $\mathcal{P}$ associating sets of

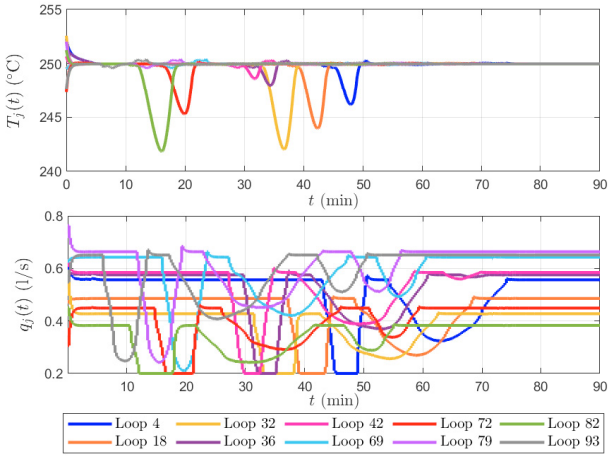

Fig. 2. Outlet temperature and HTF flow for 10 random loops when using the population dynamics-assisted coalitional approach calculating $\mathcal{P}$ in terms of DNI.

loops that receive more DNI with those that are dirty or shaded, and grouping unbalanced loops regarding their flow requirements, as in Masero et al. (2020). Without loss of generality, we consider $M = 10$ coalitions of $|\mathcal{C}_i| = 10$ loops for all $\mathcal{C}_i \in \mathcal{P}$. Moreover, we study a DNI profile with three moving clouds: a large cloud moves through the plant between $t = 3$ min and $t = 52$ min, another appears between $t = 15$ min and $t = 75$ min, and the last one crosses between $t = 40$ min and $t = 71$ min. As illustration, Fig. 1 shows the three clouds over the plant at $t = 45$ min. We also consider that some loop collectors might be cleaner than others and thus receive more radiation.

The consequences of passing clouds are shown in Fig. 2, which depicts the temporal evolution of the outlet temperature $T_j(t)$ and the HTF flow $q_j(t)$ of ten random loops. Loops that are more efficient, i.e., have less thermal losses or are cleaner, and thus receive more solar radiation, would stabilize at a higher flow value in their local operating point. For example, loops #93 (gray line) or #79 (purple line) reach a higher flow value than loops #32 (yellow line) or #82 (green line), which are less efficient. When loops are shaded, they tend to decrease their HTF flow to maintain their outlet temperature at their desired value. Consequently, less efficient loops would experience a greater drop in their outlet temperature when shaded. This issue happens because said loops stabilize at a lower flow value $q^{\circ}_j(t)$, and therefore cannot decrease their flow as much as they would like, as they saturate at $q^{\min}$.

Figure 3 presents a comparison in the evolution of the outlet temperature and the total HTF flow of the 100-loop field when applying our proposed population-dynamics-assisted coalitional MPC approach (blue-solid lines DNI clustering, and light-purple dotted-dashed lines flow clustering), a centralized controller (red-dashed lines) and an alternative coalitional approach (green-dotted lines) where the maximum flow within a coalition $q^{\max}_{\mathcal{C}_i}$ is set according to (15), and the partition $\mathcal{P}$ is calculated by asociating unbalanced loops in terms of solar irradiance. We can observe that the outlet temperature is slightly below the desired value of 250°C for more than half of the simulation, which matches the instants when the first cloud shades a larger part of the field. Although the outlet temperature

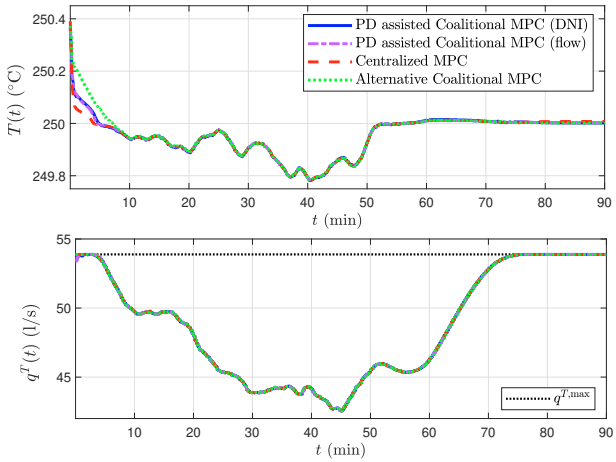

Fig. 3. Outlet temperature $T(t)$ and total HTF flow $q^T(t)$ of the 100-loop collector field. The coupled constraint $q^{T,\max}$ is represented with a black dotted line.

of the entire field suffers a small deviation regarding its desired value, the total flow of the field suffers a significant decrease. However, our proposed coalitional algorithm (resource allocation according to (14)) manages to closely follow the centralized evolution of $T(t)$ and $q^T(t)$ with a small loss in overall performance $\mathbf{P}$ of a 3.18% for the DNI clustering, and a 3.26% decrease for the flow requirement clustering. Moreover, the evolution with the alternative coalitional algorithm is further away from centralized behavior, especially at the beginning of the simulation. This results in a performance loss of 15.21% in the index $\mathbf{P}$ in relation to the centralized solution. Therefore, with the population-dynamics assistance in the allocation of the common resource, we achieve five times less performance loss than if we allocate the resource according to the operating points of the loops within a coalition (15).

Regarding the computational time, in our simulation the centralized MPC takes an average of 2.6258 ± 0.2327 s to achieve a solution. In contrast, both population-dynamics-assisted coalitional MPC require an average of 0.2623 ± 0.0087 s, and the alternative coalitional approach takes an average of 0.2614 ± 0.0152 s to obtain a solution. In this way, the coalitional control approach achieves better overall computation times, as it distributes the global problem among the set of parallel local controllers given by the partition $\mathcal{P}$ (recall that we are splitting the overall problem into $M = 10$ subproblems that are solved in parallel by independent local controllers). Hence, the benefits of applying a coalitional control schemes are more notable as the system becomes larger.

5. CONCLUDING REMARKS

In this paper, we propose a coalitional model predictive control approach for parabolic-trough plants that allows us to split the global large-scale optimization problem into smaller local subproblems. These local optimization problems remain coupled to each other through a shared resource constraint. To overcome such an issue, a population-dynamics-based resource allocation method is formulated. The proposed approach allows us to satisfy the coupled constraint while reducing the computational burden and obtaining a negligible performance loss with respect to the conventional centralized MPC approach. Further research should focus on applying this idea to larger solar plants and adapting the method to work with more complex nonlinear models.

REFERENCES

Barreiro-Gomez, J. and Tembine, H. (2018). Constrained evolutionary games by using a mixture of imitation dynamics. *Automatica*, 97, 254–262.

Barreiro-Gomez, J. and Zhu, Q. (2022). Coalitional stochastic differential games for networks. *IEEE Control Systems Letters*, 6, 2707–2712.

Camacho, E.F., Berenguel, M., and Rubio, F.R. (1997). *Advanced Control of Solar Plants*. Springer London, London.

Camacho, E.F. and Gallego, A.J. (2015). Model predictive control in solar trough plants: A review. *IFAC-PapersOnLine*, 48(23), 278–285. 5th IFAC Conference on Nonlinear Model Predictive Control NMPC 2015.

Escaño, J.M., Gallego, A.J., Sánchez, A.J., Yebra, L.J., and Camacho, E.F. (2021). Nonlinear fuzzy model predictive control of the tcp-100 parabolic trough plant. In *Joint Proceedings of the 19th World Congress of the International Fuzzy Systems Association (IFSA), the 12th Conference of the European Society for Fuzzy Logic and Technology (EUSFLAT), and the 11th International Summer School on Aggregation Operators (AGOP)*, 235–241. Atlantis Press.

Gálvez-Carrillo, M., De Keyser, R., and Ionescu, C. (2009). Nonlinear predictive control with dead-time compensator: Application to a solar power plant. *Solar Energy*, 83(5), 743–752.

Martinez-Piazuelo, J., Quijano, N., and Ocampo-Martinez, C. (2022). Nash equilibrium seeking in full-potential population games under capacity and migration constraints. *Automatica*, 141, 110285.

Masero, E., D. Frejo, J.R., Maestre, J., and Camacho, E. (2020). A light clustering model predictive control approach to maximize thermal power in solar parabolic-trough plants. *Solar Energy*, 214, 531–541.

Maxim, A. and Caruntu, C.F. (2022). Coalitional distributed model predictive control strategy for vehicle platooning applications. *Sensors*, 22(3), 997.

Peinado Gonzalo, A., Pliego Marugán, A., and García Márquez, F.P. (2019). A review of the application performances of concentrated solar power systems. *Applied Energy*, 255, 113893.

Quijano, N., Ocampo-Martinez, C., Barreiro-Gomez, J., Obando, G., Pantoja, A., and Mojica-Nava, E. (2017). The role of population games and evolutionary dynamics in distributed control systems: The advantages of evolutionary game theory. *IEEE Control Systems Magazine*, 37(1), 70–97.

Ruiz-Moreno, S., Frejo, J.R.D., and Camacho, E.F. (2021). Model predictive control based on deep learning for solar parabolic-trough plants. *Renewable Energy*, 180, 193–202.

Sandholm, W.H. (2010). *Population games and evolutionary dynamics*. MIT Press.

Şen, Z. (2004). Solar energy in progress and future research trends. *Progress in Energy and Combustion Science*, 30(4), 367–416.